

Redox chemistry and molybdenum burial in a Mesoproterozoic lake

K. I. Rico¹, N. D. Sheldon¹, T. M. Gallagher,^{1,2} and A. Chappaz³

¹Department of Earth and Environmental Sciences, University of Michigan, 1100 N. University Ave Rm 2534, Ann Arbor MI, 48109

²Now at: Jackson School of Geosciences, University of Texas at Austin, 2305 Speedway Stop C1160, Austin, TX, 78712

³Department of Earth and Atmospheric Sciences, Central Michigan University, ET Building 200, Mount Pleasant, MI, 48859

Corresponding Author: Nathan Sheldon (nsheldon@umich.edu)

Key Points:

- Fe, Mo, and U sediment geochemistry of the Nonesuch Formation (~1.1 Ga; USA) indicate fluctuating oxic and anoxic redox chemistry
- Mo and U covariation in the Nonesuch Formation and modern analogue sediments confirm euxinia is not necessary for moderate Mo burial
- Comparison of Nonesuch Formation and modern analogue indicates that Proterozoic lakes are unlikely to constrain atmospheric oxygen

This is the author manuscript accepted for publication and has undergone full peer review but has not been through the copyediting, typesetting, pagination and proofreading process, which may lead to differences between this version and the [Version of Record](#). Please cite this article as doi: [10.1029/2019GL083316](https://doi.org/10.1029/2019GL083316)

Abstract

While marine sediments have been used to constrain a history of redox chemistry throughout the Precambrian, far fewer data have been generated from lakes. With major biological innovations thought to have occurred in Proterozoic lakes, understanding their chemistry is critical for understanding the evolution of eukaryotic life. We use sediment geochemistry to characterize the redox conditions of the Nonesuch Formation (~1.1 Ga) and a modern analogue for the Proterozoic: the Middle Island Sinkhole (MIS) in Lake Huron (USA). Iron speciation, Mo contents, and Mo-U covariation demonstrate oxic and anoxic—euxinic—environments, with no clear indicators of enhanced biological productivity in the Nonesuch Formation. Moderate Mo enrichments observed in the Nonesuch Formation are not attributed to euxinia, but instead to an authigenic particulate shuttle. We suggest that the Fe and Mo sediment geochemistry of these lacustrine systems reflect only local water column and sediment burial conditions, and not atmospheric oxygenation.

Plain language summary

Lakes are proposed to have been critical environments for the evolution of life during the Proterozoic (~2.5 to 0.5 billion years ago). However, relatively little is known about the chemistry of ancient lakes, including the availability of oxygen for biological productivity, and how local oxygen availability can be extrapolated to understand global oxygen availability. In addition, with no lakes remaining from the Proterozoic, the only way to study ancient lakes is to use the chemistry of the sediments left behind. This study uses the sediment chemistry of elements that are sensitive to oxygen to understand oxygen availability in a Proterozoic lake environment. This data was then compared to modern lake environments with known chemistry and oxygen levels in order to interpret the results better. We found that oxygen availability in the Proterozoic lake was variable, with no clear indicators of abundant biological productivity. We conclude that ancient lake sediments only constrain the chemistry of the local environment, with no major implications for global or even regional atmospheric oxygenation.

1 Introduction

Geochemical characterizations of ancient marine sediments have been used successfully to investigate shifts in atmospheric oxygenation throughout the Precambrian (e.g. Farquhar, Bao, & Thieme, 2000). For the mid-Proterozoic, ocean redox chemistry and atmospheric oxygenation has been hotly debated, with geochemical methods indicating variable marine redox conditions, and subsequently, various interpretations of atmospheric oxygenation (e.g. Sperling et al., 2014; Planavsky et al., 2018). In comparison, fewer geochemical data have been generated from Proterozoic lakes to constrain the redox chemistry of terrestrial environments. However, there is increasing evidence that Proterozoic lakes—not oceans—may have been critical habitats for biological evolutions (e.g. the diversification of cyanobacteria and early eukaryotic life; Blank & Sánchez-Baracaldo, 2010; Strother et al., 2011; Blank, 2013). As a result, it becomes increasingly important to understand the habitats wherein these major evolutions took place. Constraining the geochemistry of Proterozoic lake environments can help to characterize the conditions wherein multicellular life may have evolved. Molybdenum (Mo), a redox-sensitive trace element, has been intensively used as a paleo redox proxy, mostly to identify periods of past anoxia (Chappaz, Glass, & Lyons, 2018; Hardisty et al., 2018). In presence of sulfide ($\Sigma S(-II) = H_2S + HS^- + S^{2-}$), Mo can be scavenged in sediment via two pathways: (1) through association with Fe-S minerals (e.g. Chappaz et al., 2014; Helz and Vorlieck, 2019) and (2)

73 through interactions with organic matter (e.g. Ar d a k a n i, Ch a p p a z, S a n e i, & M a y e r , 2016;
74 Wagner, Chappaz, & Lyons, 2017; Tessin, Chappaz, Hendy, & Sheldon, 2018). As a
75 consequence, Mo enrichments can exceed crustal levels by two orders of magnitude when $\Sigma S(-$
76 $II)$ is present within the water column (euxinia; Scott and Lyons, 2012). In addition, Mo is a
77 cofactor in many metabolic pathways and has consequently played a key role in biospheric
78 evolution (Lyons, Reinhard, & Planavsky, 2014). Geobiologically speaking, Mo is an essential
79 micronutrient strongly integrated into the nitrogen cycle, including vital roles in N_2 fixation and
80 fixed nitrogen assimilation, and is a key element limiting primary productivity in lakes
81 (Goldman, 1960; Howarth & Cole, 1985; Glass et al., 2012).

82 The relationship between geochemistry and biological evolution in Mesoproterozoic
83 lakes has been studied using the Stoer Group (1.18 Ga) of the Torridonian Supergroup, UK
84 (Parnell, Boyce, Mark, Bowden, & Spinks, 2010; Parnell, Spinks, Andrews,
85 Thayaalan, & Bowden, 2015). Based upon ample burial of Mo in Stoer Group sediments,
86 Parnell et al. (2015) concluded that oxygenation of terrestrial environments increased oxidative
87 weathering and sulfate delivery to lakes, allowing for widespread euxinia to develop and for
88 abundant nutrients that spurred enhanced biological productivity. However, Mo and Sr isotope
89 data indicate that much of the Stoer Group is marine or marine-influenced, and not strictly
90 lacustrine (Stüeken et al., 2017). Therefore, if the Stoer Group is not appropriate for
91 understanding redox chemistry Proterozoic lakes, we must consider other systems to investigate
92 Mesoproterozoic lacustrine geochemistry. Here, we examine the Fe and Mo geochemistry of the
93 Nonesuch Formation (~1.1 Ga; Figure 1a) of the Keweenaw Supergroup, as well as two modern
94 analogues for Proterozoic waters—the low-oxygen Middle Island Sinkhole (MIS) and an oxic
95 Lake Huron control site (LH; Figure 1b)—to test the conclusions made by Parnell et al. (2015)
96 and to assess whether euxinia and enhanced biological productivity were widespread during the
97 Mesoproterozoic in terrestrial environments.

99 2 Site Descriptions

100 2.1 The Nonesuch Formation

101 The Nonesuch Formation is comprised of sandstones, mudstones, and rare limestone
102 interbeds that were deposited as part of the Midcontinent Rift System (Elmore, Milavec,
103 Imbus, & Engel, 1989). This formation—which is bookended by alluvial fan and fluvial
104 depositional environments, and incorporates one or possibly a series of rift lakes (Suszek,
105 1997)—includes diverse freshwater phytoplankton microfossils (Wellman & Strother, 2015).
106 Further, the Nonesuch Formation interfingers in places with the Copper Harbor Conglomerate
107 (1.09 Ga), which features alluvial fan and fluvial facies, and lacustrine stromatolite mounds
108 (Elmore, 1983; Wilmeth, Dornbos, Isbell, & Czaja, 2014; Fedorchuk et al., 2016).
109 Therefore, there is an abundance of evidence that the Nonesuch Formation is comprised of
110 fluctuating freshwater environments, and lacks significant marine influence. This work uses
111 samples from cores DO-6, PI-2, and WPB-4 (Figure 1a), incorporating shore-proximal and shore-
112 distal lacustrine units possibly from two different lake sub-basins (Suszek, 1997). This work
113 includes samples from mudstone beds with consistent stratigraphic spacing
114 (roughly every 1–5 m) for each of these three cores. Nonesuch Formation
115 geochemical data and interpretations of redox chemistry are compared to that of core PI-1
116 (Cumming, Poulton, Rooney, & Selby, 2013), and DO-8 and WC-9 (Slotznick,
117 Swanson-Hysell, & Sperling, 2018), which also may also encompass
118 additional lake sub-basins.

119
120
121
122
123
124
125
126
127
128
129
130
131
132
133
134
135
136
137
138
139
140
141
142
143
144
145
146
147
148
149
150
151
152
153
154
155
156
157
158
159
160
161
162
163

2.2 The Middle Island Sinkhole (MIS)

Located in Lake Huron (Figure 1b), the Middle Island Sinkhole is a 23 m deep karst feature wherein low-oxygen high-sulfate groundwater seeps into the sinkhole, resulting in low (<5%) dissolved oxygen and 7.8 mM sulfate that persists 1–3 meters above the sediment-water interface (Ruberg et al. 2008). This water chemistry is comparable to proposed levels for mid-Proterozoic waters, which are inferred to have little to no oxygen (e.g. Shen, Canfield, & Knoll, 2002; Lyons et al., 2014), and sulfate concentrations in the range of <2 mM to ~10 mM (Olson, Reinhard, & Lyons, 2016; Blättler et al., 2018). As a result of this water chemistry, dynamic microbial mats grow at this interface, including cyanobacteria that conduct both oxygenic and anoxygenic photosynthesis (Voorhies et al., 2012), and are therefore similar to the versatile cyanobacteria proposed to have dominated Proterozoic aquatic systems (Johnston, Wolfe-Simon, Pearson, & Knoll, 2009; Voorhies et al., 2012). Redox chemistry of MIS allows for the burial of nutrient- and metal-rich sediments below the microbial mat (Nold et al., 2013; Kinsman-Costello et al., 2017; Rico & Sheldon, 2019). With water chemistry and microbiology similar to what has been inferred for the Proterozoic, MIS has been considered an analogue to interpret biogeochemical cycling in shallow Proterozoic waters (Voorhies et al., 2012; Kinsman-Costello et al., 2017; Rico & Sheldon, 2019).

A Lake Huron (LH) control site of comparable depth to MIS is used to provide an oxic endmember. LH, which is 0.6 km away from MIS (Figure 1b), is comprised of mudstones like MIS, but has limited groundwater influence and no evidence of a microbial mat at the sediment water interface (Kinsman-Costello et al., 2017). Porewater and sediment geochemistry, and microbial community assemblage, differ between MIS and LH (Kinsman-Costello et al., 2017; Rico & Sheldon, 2019). For MIS and LH, samples encompass surficial sediments (<25 cm depth).

3 Methods

MIS (n = 56), LH (n = 22) Mo, U, and Al contents, and Nonesuch Formation (n = 113) Mo, Fe, U, Al, S, and P concentrations were analyzed at ALS Laboratories in Vancouver, British Columbia, where samples were digested with perchloric, hydrofluoric, nitric, and hydrochloric acids, and concentrations were determined by ICP-OES and ICP-MS calibrated using internal standards. Major element precision was better than 0.2 wt.%. A single outlier for LH with respect to Mo was excluded from this work. To compare the respective enrichments of Mo and U in the study locations, trace metal concentrations are given in the form of enrichment factors (EFs), which were calculated as:

$$X_{EF} = [(X/Al)_{\text{sample}} / (X/Al)_{\text{background}}] \quad (1)$$

where X and Al represent the weight percent concentrations of elements X and Al, respectively. For the Nonesuch Formation, samples are normalized using the post-Archean average shale (PAAS) compositions of Taylor and McLennan (1985). LH and MIS samples were normalized using average Lake Huron background values of Mo (0.25 ± 0.05 ppm), U (1.02 ± 0.15 ppm), and Al (3.1 ± 1.1 wt. %; after Chappaz, Gobeil, & Tessier, 2008). While there are potential pitfalls with any normalization (e.g. PAAS may not be representative of local sediments; Van der Weijden, 2002), because this study aims to compare respective enrichments of Mo and U, the

164 differences in reference material between our study sites should not have major implications for
165 our overall interpretations.

166 For total organic carbon (TOC) analyses, Nonesuch Formation samples (n = 112) were
167 washed with a 1–2N HCl solution to remove carbonates, rinsed, and oven-dried overnight at
168 50°C. In order to get TOC of the bulk sample, acidified and unacidified sample pairs were loaded
169 into tin capsules, and analyzed using a Costech ECS4010 elemental analyzer in UM’s Earth
170 System Science Lab. Acetanilide (%C = 71.09, %N = 10.36) was used to calibrate elemental
171 composition.

172 Fe speciation for the Nonesuch Formation (n = 55) samples was determined using a
173 three-step sequential extraction developed by Poulton and Canfield (2005). Pyrite concentrations
174 were stoichiometrically determined via titration of chromium reducible sulfide precipitated as
175 ZnS (Canfield, Raiswell, Westrich, Reaves, & Berner, 1986). The total highly reactive
176 pool of iron (iron that is highly reactive towards sulfide; Fe_{HR}; Poulton & Canfield, 2005)
177 represents the sum of these four extractions. Detailed methods are given in Table S1 in the
178 supporting information. Iron in the Nonesuch Formation sequential extraction solutions were
179 analyzed by ICP-MS within the STARLAB at Central Michigan University. Uncertainties for all
180 Fe pools were less than 0.2 wt. %. All of the sediment geochemical data (this work) are
181 presented in Tables S2–S3 in the Data Repository.

182 To calibrate “normal” distributions of Mo and U in large lakes, water column samples
183 were collected at three stations in August 2014 at 10 different depths using Niskin bottles aboard
184 R/V Blue Heron in Lake Superior. Within 1 hour and in a clean environment, all water samples
185 were filtered with 0.45 µm syringe nylon filters and transferred into 50 mL HDPE (previously
186 acid washed) tubes filled with 1 mL of HNO₃ high purity (Optima, 2% v/v). Molybdenum and U
187 concentrations were determined at the STARLAB at Central Michigan University using ICP-MS
188 analysis and external calibration.

190 **4 Results and Discussion**

191 4.1 Redox chemistry of the Nonesuch Formation

192 Analysis of Fe speciation uses Fe_{HR}/Fe_T and Fe_{py}/Fe_{HR} to differentiate between oxic,
193 ferruginous (Fe(II) within the water column), anoxic ($\Sigma S(-II)$ only present in the porewater) and
194 euxinic conditions (e.g. Tessin, Sheldon, Hendy, & Chappaz, 2016). Previous Fe speciation data
195 for the Nonesuch Formation from a nearby core (Figure 1) to the ones examined herein indicate
196 predominantly ferruginous conditions (Cumming et al., 2013; Figure S1). In contrast, magnetic
197 Fe mineralogy and petrographic data from two cores in Northern Wisconsin have been
198 interpreted to indicate that the Nonesuch Formation there featured oxic water columns (Slotznick
199 et al., 2018). Thus, one possibility for this discrepancy is that the proxies are not reliably
200 recording water column oxygenation. However, modern sequential Fe extraction results
201 appropriately define MIS as ferruginous and LH as oxic (Figure 2; Rico & Sheldon, 2019),
202 matching their known oxygen levels, so we consider the Fe-based proxies to be reliable. The new
203 Nonesuch Formation data mostly indicate oxic or possibly anoxic conditions (Figure 2), with
204 significant overlap between individual cores (DO-6, PI-2, WPB-4; Figure S1). Notably, Fe
205 speciation results indicate that the oxic LH sediments are more anoxic than the majority of the
206 Nonesuch Formation samples. This is driven by an Fe limitation in LH; there is a much higher
207 relative abundance (~5x LH) of Fe_T in the Nonesuch Formation. As cautioned by Raiswell et al.
208 (2018), this work suggests that discrepancies in local Fe enrichments need to be considered when
209 comparing Fe speciation results for spatially or temporally separate aquatic systems.

210 Iron speciation results for much of the Nonesuch Formation sediments indicate a high
211 degree of pyritization with oxic deposition (Figure 2), which is rare for modern systems (Tables
212 S2 and S3). However, especially with limited oxygen availability in the mid-Proterozoic (e.g.
213 Planavsky et al., 2018), reduced chemical species such as pyrite are to be expected when oxygen
214 is consumed. In contrast, MIS does not display a high degree of pyritization, likely attributed to a
215 sulfide limitation in porewater (which fluctuates between 0–7 mM H₂S; Kisman-Costello et al.,
216 2017). Given that the Nonesuch Formation is likely comprised of a series of rift basins (Suszek,
217 1997), data from this study could incorporate separate lake systems that overlap with those of
218 previously published data from Cumming et al. (2013) and Slotznick et al. (2018). Taken
219 together, variability in interpretations of Fe geochemistry in the Nonesuch Formation could in
220 part reflect real spatial and temporal variability in water chemistries and depths of the
221 sedimentary environments.

222 223 4.2 Molybdenum burial in the Nonesuch Formation

224 The modern anoxic analogue and oxic lake sediments exhibit a large range in organic C
225 contents (0.3–10.4%), whereas their Mo contents are consistently low (<1 ppm; Figure 3),
226 regardless of redox conditions. In comparison, the Nonesuch Formation samples exhibit a
227 smaller range in organic C (0–1.7%) but feature higher Mo concentrations (0.12–40 ppm; Figure
228 3). However, both the modern systems and the Nonesuch Formation exhibit Mo contents far
229 below what is anticipated for euxinic conditions (e.g. as in the Stoer Group; Figure 3).

230 The highest accumulation of authigenic Mo is conventionally attributed to the presence of
231 free sulfide ($\Sigma S(-II)$; i.e. euxinic conditions) and subsequent formation of thiomolybdates
232 (Erickson & Helz, 2000; Vorlicek et al., 2015). Some Nonesuch Formation samples exhibit Mo
233 enrichments relative to the modern systems (Figure 3), yet there is no evidence for persistent
234 euxinia in any of the lake environments (Table 1; Figures 2 and 3). To refine the mechanisms
235 that could control Mo burial, the Mo-U covariation was evaluated across all of our sites.

236 Trends in Mo-U covariation for modern and ancient marine systems have been linked to
237 the controls on Mo deposition in sediments (Algeo & Tribovillard, 2009; Tribovillard,
238 Algeo, Baudin, & Ribouilleau, 2012). Molybdenum enrichments can occur: 1) via a
239 “particulate shuttle” wherein authigenic Mo is scavenged by metal hydroxides (e.g. Mn and Fe),
240 transported through the water column, and buried in sediments (authigenic U does not get
241 scavenged in this process, resulting in a high Mo_{EF} and comparably low U_{EF}) or 2) via a shift
242 from suboxic to anoxic to euxinic water chemistry, enabling an enrichment in U under suboxia,
243 and then enhanced burial of Mo in the presence of free sulfide (i.e. the “unrestricted marine”
244 trend wherein U_{EF} increases then Mo_{EF} increases; Algeo & Tribovillard, 2009). The Mo_{EF}/U_{EF}
245 method uses mass ratios from modern seawater to designate threshold concentrations that can be
246 related to depositional processes. Average seawater concentrations for Mo and U are 10.6 and
247 3.1 ppb, respectively (Mo/U = 3.4 Algeo & Tribovillard, 2009). Throughout the entire water
248 column at three different stations in Lake Superior (max depth of 315 m), average concentrations
249 for Mo and U are 0.13 and 0.04 ppb, respectively (n = 30; Mo/U = 3.3; Table S4). Given that the
250 Mo_{EF}/U_{EF} method is based on ratios (not total concentration), the fact that Mo/U_{seawater} is almost
251 identical to the Mo/U_{Lake Superior} (3.4 vs. 3.3) implies that the approach developed by Algeo and
252 Tribovillard (2009) can be applied to our lacustrine systems.

253 As a fully oxygenated system, LH sediments are anticipated to have little Mo and U
254 enrichment; this is corroborated by low EFs in Figure 4. MIS sediments are more enriched in Mo
255 and U relative to LH sediments, with no overlap, and may follow the “particulate shuttle”

256 pathway of Mo burial (Figure 3). In comparison, ~30% of the Nonesuch Formation data are
257 enriched (EF > 1) for Mo and U, with only a few samples exhibiting substantial enrichment (EF
258 > 10). However, the samples that are enriched fall along the “particulate shuttle” pathway
259 (Figure 4). This suggests that for the Nonesuch Formation, euxinic conditions are not directly
260 causing Mo enrichments. Instead, the dominant burial mechanism for Mo is the “particulate
261 shuttle” pathway; enrichments in Fe_T and Fe_{ox} (Table S3) may have favored Mo enrichments via
262 this pathway relative to MIS and LH.

263

264 4.3 Implications for biological productivity and atmospheric oxygen

265 Based upon sediment Mo geochemistry in the Mesoproterozoic Stoer Group, Parnell et al. (2015)
266 hypothesized that high atmospheric pO_2 in the Mesoproterozoic would have increased delivery
267 of sulfate, resulting in 1) sulfate reduction and significant Mo burial via sulfides in lakes (i.e.
268 widespread euxinia), and 2) no nutrient limitation and therefore high levels of biological
269 productivity. While the Stoer Group is marine-influenced, and not strictly lacustrine (Stüeken et
270 al., 2017), Parnell et al. (2015) provide a testable hypothesis for Mesoproterozoic lake
271 environments. The Stoer Group Mo contents are greater than both those of the Nonesuch
272 Formation and the modern systems (Figure 3) and could be the result of post depositional
273 processes remobilizing and enriching Mo (e.g. Ardakani et al., 2016). When combining our
274 different approaches (Fe speciation and Mo-U covariation), there is no evidence that euxinia was
275 widespread across terrestrial environments during the Mesoproterozoic, nor any clear indicators
276 for abundant nutrient availability that would help to sustain biological activity (Figures 2 and 4).
277 The Nonesuch Formation sediments feature organic C contents similar to a modern biologically
278 productive environment (LH; Figure 3) and experienced a relatively mild thermal history (<150
279 °C; Gallagher et al., 2017) suggesting that their C contents are not substantially lower than they
280 were at the time of deposition. However, it is unclear whether this organic C burial can be
281 attributed to an increase in biological productivity or a shift to greater carbon preservation. Well-
282 preserved eukaryotic remains are most abundant and diverse in discrete horizons, which may
283 indicate that pelagic productivity occurred in episodic bursts (Wellman & Strother, 2015), but do
284 not correspond to the observed Mo enrichments. This would be consistent with intermittent
285 nutrient limitation, impacting the extent of biological productivity, and ultimately contrasting
286 with the model of Parnell et al. (2015). Without high enough Mo to indicate significant sulfate
287 weathering, this study provides no clear indicator of Mesoproterozoic atmospheric oxygenation
288 levels. Differences were observed in Fe geochemistry between various Nonesuch Formation rift
289 basin lakes and in the apparent degree of oxygenation from anoxic to oxic. This variability
290 occurred in sediments that were formed penecontemporaneously and therefore under
291 approximately the same atmospheric pO_2 , indicating that oxygen availability was locally
292 controlled in the water column and sediments (e.g. by biological production and consumption of
293 oxygen, or physically via stratification) rather than by the atmosphere. In the modern analogue
294 setting, an oxygenated atmosphere coexists with both oxic and ferruginous sediment chemistry
295 (Table 1). Taking all of this together, the most parsimonious explanation of the Nonesuch
296 Formation Mo geochemistry is that it reflects fluctuating redox conditions and intense cycling of
297 Fe and Mn oxyhydroxides within the water column, raising questions about attempts to use
298 ancient lakes to reconstruct atmospheric oxygen levels. Indeed, the modern analogue system
299 records ferruginous conditions reflective of a steep redoxcline at depth even in a fully
300 oxygenated atmosphere and thus reflects only a portion of the water column, and not the part that
301 is in contact with the atmosphere.

302
303
304
305
306
307
308
309
310
311
312
313
314
315
316
317
318
319
320
321
322
323
324

5 Conclusions

It has been proposed that Mo enrichments in Mesoproterozoic lake deposits would indicate widespread euxinia, no nutrient limitation in terrestrial systems, and high levels of atmospheric oxygen. Iron speciation, low Mo contents, and Mo-U covariation of the 1.1 Ga old Nonesuch Formation contradict this model of widespread lacustrine euxinia, and do not provide any indication of enhanced biological productivity or provide a useful constraint on atmospheric oxygenation during the Mesoproterozoic. Sediment geochemistry of Proterozoic terrestrial environments may only demonstrate *in situ* water column and sediment chemistry. Whether or not Mo geochemistry of Mesoproterozoic lakes record biological productivity and global atmospheric oxygenation remains unresolved.

Acknowledgements

We acknowledge the National Oceanic Administration Thunder Bay National Marine Sanctuary (NOAA TBNMS) scuba divers for their expertise and assistance in the collection of sediment cores at MIS and LH. We would also like to thank both the Wisconsin Geologic & Natural History Survey and the Northern Michigan Geological Repository for providing access to core material. This work was supported by National Science Foundation Graduate Student Research Fellowships to KIR and TMG, and a Sokol Foundation grant to NDS. Data supporting the conclusions (for Figures 2–4) can be obtained from supporting information (Figures S1–S3 and Tables S1–S4).

325 **References**

- 326 Algeo, T. J., & Tribovillard, N. (2009). Environmental analysis of paleoceanographic systems
327 based on molybdenum-uranium covariation. *Chemical Geology*, 268(3–4), 211–225.
328 <http://doi.org/10.1016/j.chemgeo.2009.09.001>
- 329 Ardakani, O. H., Chappaz, A., Sanei, H., & Mayer, B. (2016). Effect of thermal maturity on
330 remobilization of molybdenum in black shales. *Earth and Planetary Science Letters*, 449,
331 311–320. <http://doi.org/10.1016/j.epsl.2016.06.004>
- 332 Asael, D., Isson, T. T., Riedinger, N., Lyons, T. W., Aller, R. C., Hardisty, D. S., ... Johnston, D.
333 T. (2018). An evaluation of sedimentary molybdenum and iron as proxies for pore fluid
334 paleoredox conditions. *American Journal of Science*, 318(5), 527–556.
335 <http://doi.org/10.2475/05.2018.04>
- 336 Blättler, C.L., Claire, M.W., Prave, A.R., Kirsimäe, K., Higgins, J.A., Medvedev, P. V.,
337 Romashkin, A.E., Rychanchik, D. V., Zerkle, A.L., Paiste, K., Kreitsmann, T., Millar, I.L.,
338 Hayles, J.A., Bao, H., Turchyn, A. V., Warke, M.R., & Lepland, A. (2018). Two-billion-
339 year-old evaporites capture Earth's great oxidation. *Science*, 360, 320–323.
340 <https://doi.org/10.1126/science.aar2687>
- 341 Canfield, D. E., Poulton, S. W., Knoll, A. H., Narbonne, G. M., Ross, G., Goldberg, T., &
342 Strauss, H. (2008). Ferruginous Condition Dominated Later Neoproterozoic Deep Water
343 Chemistry. *Science*, 321(August), 949–952. <http://doi.org/10.1126/science.1154499>
- 344 Canfield, D. E., Raiswell, R., Westrich, J. T., Reaves, C. M., & Berner, R. A. (1986). The use of
345 chromium reduction in the analysis of reduced inorganic sulfur in sediments and shales.
346 *Chemical Geology*, 54(1–2), 149–155. [http://doi.org/10.1016/0009-2541\(86\)90078-1](http://doi.org/10.1016/0009-2541(86)90078-1)
- 347 Chappaz, A., Glass, J., Lyons, T. W. (2018). Molybdenum. In W. M. White, W. H. Casey, B.
348 Marty, H. Yurimoto. *Encyclopedia of Geochemistry* v. 2, (pp. 947–950). Cham,
349 Switzerland: Springer International.
- 350 Chappaz, A., Gobeil, C., & Tessier, A. (2008). Geochemical and anthropogenic enrichments of
351 Mo in sediments from perennially oxic and seasonally anoxic lakes in Eastern Canada.
352 *Geochimica et Cosmochimica Acta*, 72(1), 170–184.
353 <http://doi.org/10.1016/j.gca.2007.10.014>
- 354 Chappaz, A., Lyons, T. W., Gregory, D. D., Reinhard, C. T., Gill, B. C., Li, C., & Large, R. R.
355 (2014). Does pyrite act as an important host for molybdenum in modern and ancient euxinic
356 sediments? *Geochimica et Cosmochimica Acta*, 126, 112–122.
357 <http://doi.org/10.1016/j.gca.2013.10.028>
- 358 Cumming, V. M., Poulton, S. W., Rooney, A. D., & Selby, D. (2013). Anoxia in the terrestrial
359 environment during the late Mesoproterozoic. *Geology*, 41(5), 583–586.
360 <http://doi.org/10.1130/G34299.1>

- 361 Elmore, R. D., Milavec, G. J., Imbus, S. W., & Engel, M. H. (1989). The Precambrian nonesuch
362 formation of the North American mid-continent rift, sedimentology and organic
363 geochemical aspects of lacustrine deposition. *Precambrian Research*, 43(3), 191–213.
364 [http://doi.org/10.1016/0301-9268\(89\)90056-9](http://doi.org/10.1016/0301-9268(89)90056-9)
- 365 Elmore, R. D. (1983). Precambrian non-marine stromatolites in alluvial fan deposits, the Copper
366 Harbor Conglomerate, upper Michigan. *Sedimentology*, 30(6), 829–842.
367 <http://doi.org/10.1111/j.1365-3091.1983.tb00713.x>
- 368 Falkowski, P. G., Katz, M. E., Knoll, A. H., Quigg, A., Raven, J. A., Schofield, O., & Taylor, F.
369 J. R. (2004). The evolution of modern eukaryotic phytoplankton. *Science*, 305(July), 354–
370 360. <http://doi.org/10.1126/science.1095964>
- 371 Farquhar, J., Bao, H., & Thiemens, M. (2000). Atmospheric Influence of Earth's Earliest Sulfur
372 Cycle. *Science*, 289, 756–758. <http://doi.org/10.1126/science.289.5480.756>
- 373 Fedorchuk, N. D., Dornbos, S. Q., Corsetti, F. A., Isbell, J. L., Petryshyn, V. A., Bowles, J. A., &
374 Wilmeth, D. T. (2016). Early non-marine life: Evaluating the biogenicity of
375 Mesoproterozoic fluvial-lacustrine stromatolites. *Precambrian Research*, 275, 105–118.
376 <http://doi.org/10.1016/j.precamres.2016.01.015>
- 377 Gallagher, T. M., Sheldon, N. D., Mauk, J. L., Petersen, S. V., Gueneli, N., & Brocks, J. J.
378 (2017). Constraining the thermal history of the North American Midcontinent Rift System
379 using carbonate clumped isotopes and organic thermal maturity indices. *Precambrian*
380 *Research*, 294, 53–66. <http://doi.org/10.1016/j.precamres.2017.03.022>
- 381 Helz, G. R., & Vorliceck, T. P. (2019). Precipitation of molybdenum from euxinic waters; role of
382 organic matter. *Chemical Geology*, 509(January), 178–193.
383 <http://doi.org/10.1016/j.chemgeo.2019.02.001>
- 384 Johnston, D. T., Wolfe-Simon, F., Pearson, A., & Knoll, A. H. (2009). Anoxygenic
385 photosynthesis modulated Proterozoic oxygen and sustained Earth's middle age.
386 *Proceedings of the National Academy of Sciences*, 106(40), 16925–16929.
387 <http://doi.org/10.1073/pnas.0909248106>
- 388 Kinsman-Costello, L. E., Sheik, C. S., Sheldon, N. D., Burton, G. a., Costello, D., Marcus, D. N.,
389 ... Dick, G. J. (2017). Groundwater shapes sediment biogeochemistry and microbial
390 diversity in a submerged sinkhole. *Geobiology*, 15(2), 225–239.
391 <http://doi.org/10.1038/nature04068>
- 392 Lyons, T. W., Reinhard, C. T., & Planavsky, N. J. (2014). The rise of oxygen in Earth's early
393 ocean and atmosphere. *Nature*, 506(7488), 307–15. <http://doi.org/10.1038/nature13068>
- 394 März, C., Poulton, S. W., Beckmann, B., Küster, K., Wagner, T., & Kasten, S. (2008). Redox
395 sensitivity of P cycling during marine black shale formation: Dynamics of sulfidic and

- 396 anoxic, non-sulfidic bottom waters. *Geochimica et Cosmochimica Acta*, 72(15), 3703–3717.
397 <http://doi.org/10.1016/j.gca.2008.04.025>
- 398 Nold, S. C., Bellecourt, M. J., Kendall, S. T., Ruberg, S. A., Sanders, T. G., Klump, J. V., &
399 Biddanda, B. A. (2013). Underwater sinkhole sediments sequester Lake Huron's carbon.
400 *Biogeochemistry*, 115(1–3), 235–250. <http://doi.org/10.1007/s10533-013-9830-8>
- 401 Olson, S.L., Reinhard, C.T., & Lyons, T.W. (2016). Limited role for methane in the mid-
402 Proterozoic greenhouse. *Proceedings of the National Academy of the Sciences*, 113(41), 2–
403 7. <http://doi.org/10.1073/pnas.1608549113>
- 404 Parnell, J., Boyce, A. J., Mark, D., Bowden, S., & Spinks, S. (2010). Early oxygenation of the
405 terrestrial environment during the Mesoproterozoic. *Nature*, 468(7321), 290–293.
406 <http://doi.org/10.1038/nature09538>
- 407 Parnell, J., Spinks, S., Andrews, S., Thayalan, W., & Bowden, S. (2015). High Molybdenum
408 availability for evolution in a Mesoproterozoic lacustrine environment. *Nature*
409 *Communications*, 6, 6996. Retrieved from <https://doi.org/10.1038/ncomms7996>
- 410 Planavsky, N. J., Slack, J. F., Cannon, W. F., O'Connell, B., Isson, T. T., Asael, D., ... Bekker,
411 A. (2018). Evidence for episodic oxygenation in a weakly redox-buffered deep mid-
412 Proterozoic ocean. *Chemical Geology*, 483(August 2017), 581–594.
413 <http://doi.org/10.1016/j.chemgeo.2018.03.028>
- 414 Poulton, S., & Canfield, D. E. (2005). Development of a sequential extraction procedure for iron:
415 implications for iron partitioning in continentally derived particulates. *Chemical Geology*,
416 214(3–4), 209–221. <http://doi.org/10.1016/j.chemgeo.2004.09.003>
- 417 Raiswell R., & Canfield D.E. (2012) The iron biogeochemical cycle past and present.
418 *Geochemical Perspectives*, 1, 1–220.
- 419 Raiswell, R., Hardisty, D. S., Lyons, T. W., Canfield, D. E., Owens, J. D., Planavsky, N. J., ...
420 Reinhard, C. T. (2018). The iron paleoredox proxies: A guide to the pitfalls, problems and
421 proper practice. *American Journal of Science*, 318(5), 491–526.
422 <http://doi.org/10.2475/05.2018.03>
- 423 Rico, K. I., & Sheldon, N. D. (2019). Nutrient and iron cycling in a modern analogue for the
424 redoxcline of a Proterozoic ocean shelf. *Chemical Geology*, 511, 42–50.
425 <http://doi.org/10.1016/j.chemgeo.2019.02.032>
- 426 Ruberg, S. A., Kendall, S. T., Biddanda, B. A., Black, T., Nold, S. C., Lusardi, W. R., ...
427 Constant, S. A. (2008). Observations of the Middle Island Sinkhole and Glacial Creation of
428 400 Million Years. *Marine Technology Society Journal*, 42(4), 12–21.

- 429 Scott, C., & Lyons, T. W. (2012). Contrasting molybdenum cycling and isotopic properties in
430 euxinic versus non-euxinic sediments and sedimentary rocks: Refining the paleoproxies.
431 *Chemical Geology*, 324–325, 19–27. <http://doi.org/10.1016/j.chemgeo.2012.05.012>
- 432 Shen, Y., Canfield, D.E., & Knoll, A.H. (2002). Middle Proterozoic ocean chemistry: evidence
433 from the McArthur Basin, Northern Australia. *American Journal of Science*, 302, 1–27.
434 <http://doi.org/10.1126/science.3.53.32>
- 435 Slotznick, S. P., Swanson-Hysell, N. L., & Sperling, E. A. (2018). Oxygenated Mesoproterozoic
436 lake revealed through magnetic mineralogy. *Proceedings of the National Academy of*
437 *Sciences*, 201813493. <http://doi.org/10.1073/pnas.1813493115>
- 438 Stüeken, E. E., Bellefroid, E. J., Prave, A., Asael, D., Planavsky, N. J., & Lyons, T. W. (2017).
439 Not so non-marine? Revisiting the Stoer Group and the Mesoproterozoic biosphere.
440 *Geochemical Perspectives Letters*, 3(3), 221–229. <http://doi.org/10.7185/geochemlet.1725>
- 441 Suszek, T. (1997). Petrography and sedimentation of the middle Proterozoic (Keweenawan)
442 Nonesuch Formation, western Lake Superior region, Midcontinent Rift System. In
443 R.W. Ojakangas, A.B. Dickas, J. C. Green (Eds.), *Middle Proterozoic to Cambrian Rifting,*
444 *Central North American* (pp. 195–210). Geological Society of America Special Papers.
- 445 Taylor, S. R., & McLennan, S. M. (1985). *The continental crust: Its composition and evolution,*
446 Oxford, UK: Blackwell.
- 447 Tessin, A., Chappaz, A., Hendy, I., & Sheldon, N. (2018). Molybdenum speciation as a paleo-
448 redox proxy: A case study from Late Cretaceous Western Interior Seaway black shales.
449 *Geology*, 47(1), 59–62. <http://doi.org/10.1130/g45785.1>
- 450 Tessin, A., Sheldon, N. D., Hendy, I., & Chappaz, A. (2016). Iron limitation in the Western
451 Interior Seaway during the Late Cretaceous OAE 3 and its role in phosphorus recycling and
452 enhanced organic matter preservation. *Earth and Planetary Science Letters*, 449, 135–144.
453 <http://doi.org/10.1016/j.epsl.2016.05.043>
- 454 Tribovillard, N., Algeo, T. J., Baudin, F., & Riboulleau, A. (2012). Analysis of marine
455 environmental conditions based on molybdenum-uranium covariation-Applications to
456 Mesozoic paleoceanography. *Chemical Geology*, 324–325, 46–58.
457 <http://doi.org/10.1016/j.chemgeo.2011.09.009>
- 458 Van der Weijden, C.H. (2002). Pitfalls of normalization of marine geochemical data using a
459 common divisor. *Marine Geology*. 184, 167–187.
- 460 Voorhies, A. A., Biddanda, B. A., Kendall, S. T., Jain, S., Marcus, D. N., Nold, S. C., ... Dick,
461 G. J. (2012). Cyanobacterial life at low O₂: community genomics and function reveal
462 metabolic versatility and extremely low diversity in a Great Lakes sinkhole mat.
463 *Geobiology*, 10(3), 250–67. <http://doi.org/10.1111/j.1472-4669.2012.00322.x>

464 Wagner, M., Chappaz, A., & Lyons, T. W. (2017). Molybdenum speciation and burial pathway
465 in weakly sulfidic environments: Insights from XAFS. *Geochimica et Cosmochimica Acta*,
466 206, 18–29. <http://doi.org/10.1016/j.gca.2017.02.018>

467 Wellman, C. H., & Strother, P. K. (2015). The terrestrial biota prior to the origin of land plants
468 (embryophytes): A review of the evidence. *Palaeontology*, 58(4), 601–627.
469 <http://doi.org/10.1111/pala.12172>

470 Wilmeth, D. T., Dornbos, S. Q., Isbell, J. L., & Czaja, A. D. (2014). Putative domal microbial
471 structures in fluvial siliciclastic facies of the Mesoproterozoic (1.09 Ga) Copper Harbor
472 Conglomerate, Upper Peninsula of Michigan, USA. *Geobiology*, 12(1), 99–108.
473 <http://doi.org/10.1111/gbi.12071>

474

475

476

477

Table 1. Percentage of Fe speciation data indicative of a given redox regime

Location	Percent oxic (%)	Percent possibly anoxic (%; ancient sediments only)	Percent ferruginous (%)	Percent possibly euxinic (%)	Percent euxinic (%)
Middle Island Sinkhole	16	--	78	5	0
Lake Huron	100	--	0	0	0
Nonesuch Formation	73(40) ¹	25(45)	0(14)	0	<1(<1)

¹Values are given for MIS, LH, and the Nonesuch Formation from *this work*, with parenthetical values including both *this work* and previously published data from Cumming et al. (2013; Figure S1).

478

479

480

481

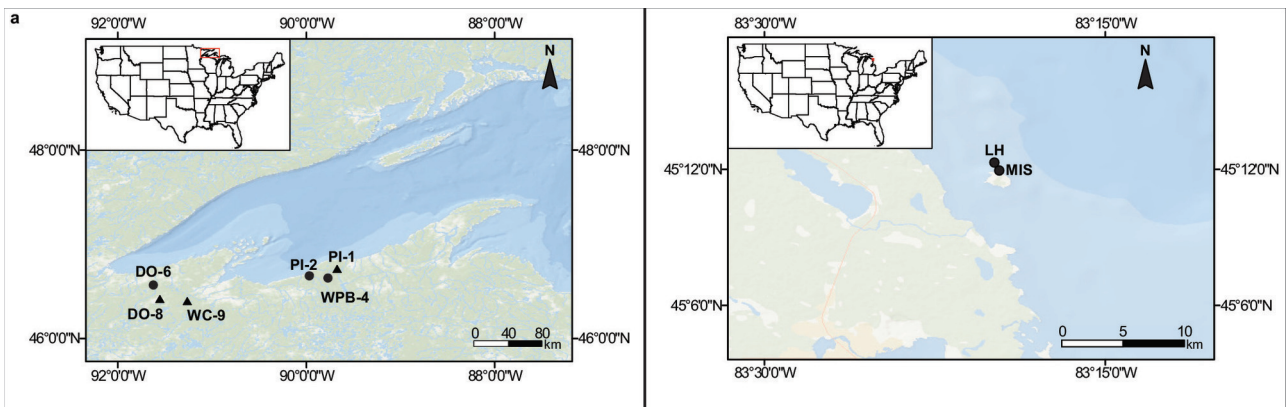
482 **Figure 1.** Sample localities for the a) DO-6, PI-2, and WPB-4 cores of the
483 Nonesuch Formation and b) Middle Island Sinkhole (MIS) and Lake Huron
484 control site (LH). The PI-1 core was previously examined for Fe speciation
485 by Cumming et al. (2013), and the DO-8 and WC-9 cores were previously
486 examined by Slotznick et al. (2018).

487
488 **Figure 2.** Cross plot of the ratios of iron in pyrite (Fe_{py}) to highly reactive iron (Fe_{HR}) versus
489 Fe_{HR} to total iron (Fe_T) for Middle Island Sinkhole (dark blue circles) Lake Huron (yellow
490 circles), and Nonesuch Formation (red circles) sediments. These Fe ratios can distinguish the
491 redox chemistries of aquatic environments as oxic, ferruginous, or euxinic (Raiswell and
492 Canfield, 2012; Raiswell et al., 2018). Solid gray lines are recommended boundaries whereas
493 dashed gray line is suggested only for ancient sediments (after Raiswell et al., 2018). Middle
494 Island Sinkhole and Lake Huron data is from Rico and Sheldon (2019).

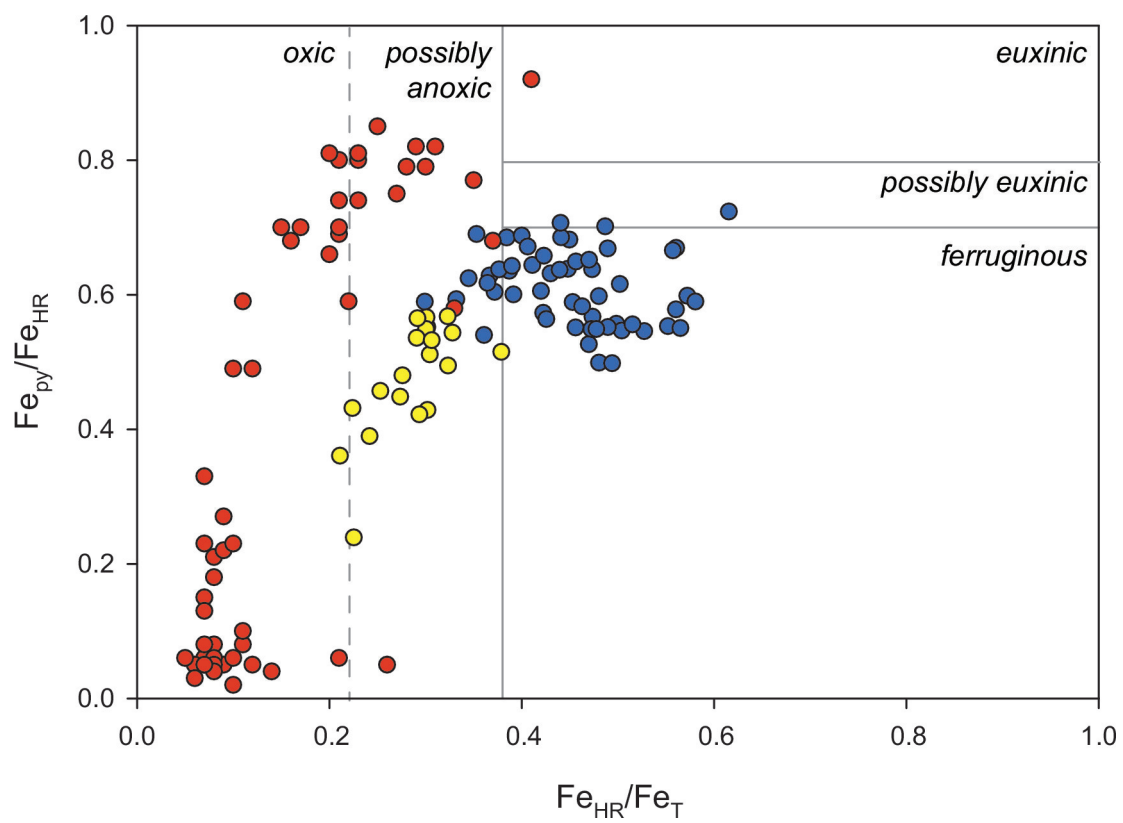
495
496 **Figure 3.** Mo (ppm) versus $\%C_{org}$ contents for Middle Island Sinkhole (blue circles), Lake
497 Huron (yellow circles), and Nonesuch Formation (red circles). Stoer Group data (gray circles;
498 Parnell et al., 2015) are also included as a comparative euxinic endmember. Dashed lines
499 indicate thresholds for oxic, anoxic, and euxinic conditions based upon Mo enrichments (Scott
500 and Lyons, 2012). Inset plot highlights Lake Huron and Nonesuch Formation data. Middle Island
501 Sinkhole and Lake Huron organic C data is from Rico and Sheldon (2019).

502 **Figure 4.** Cross plot of the enrichment factors (EFs) of Mo and U for the Nonesuch Formation
503 sediments (red circles), MIS sediments (blue field) and Lake Huron sediments (yellow field) for
504 samples enriched in Mo and U relative to their reference value ($EF > 1$). Diagonal lines represent
505 the Mo:U ratio of present-day seawater and fractions thereof. Large arrows depict the particulate
506 shuttle and unrestricted marine pathways of Mo and U deposition in marine sediments. Similar
507 Mo/U ratios between Lake Superior (3.3) and average seawater (3.4) allow us to use this marine
508 approach (after Algeo & Tribouillard, 2009) with the lacustrine sediments.

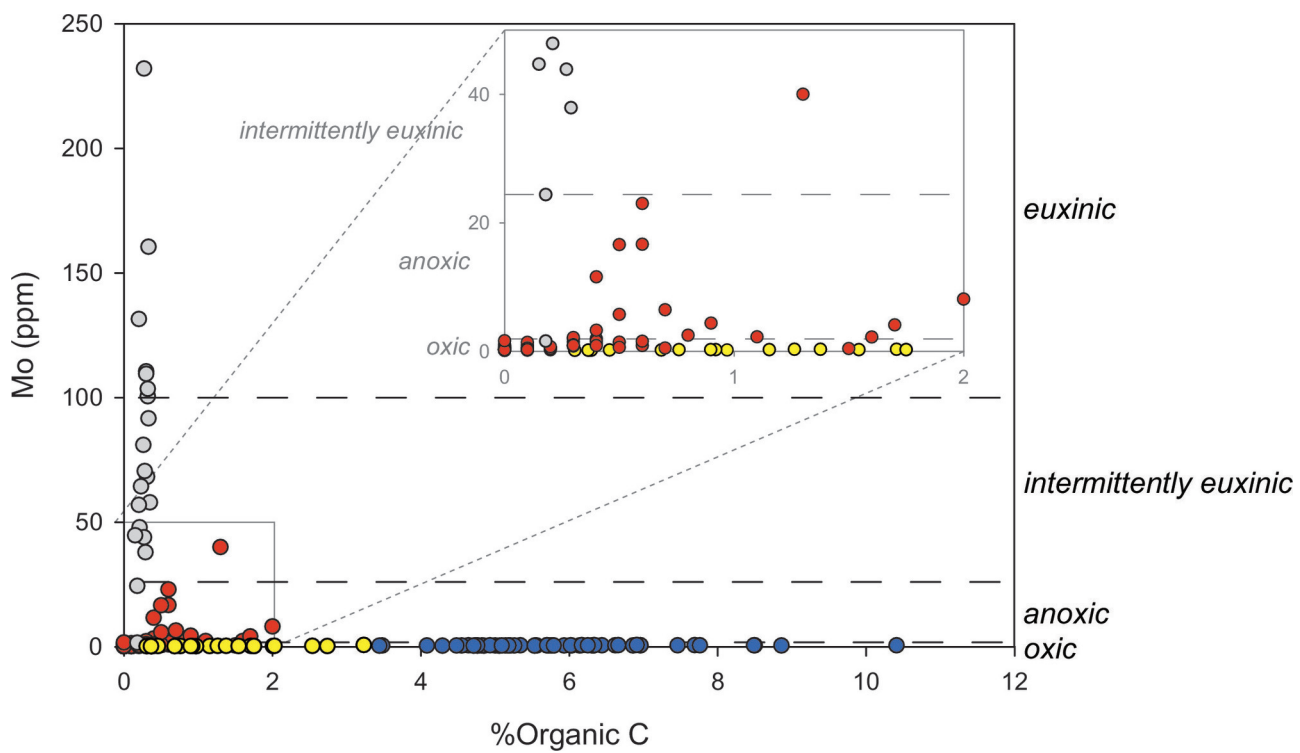
509



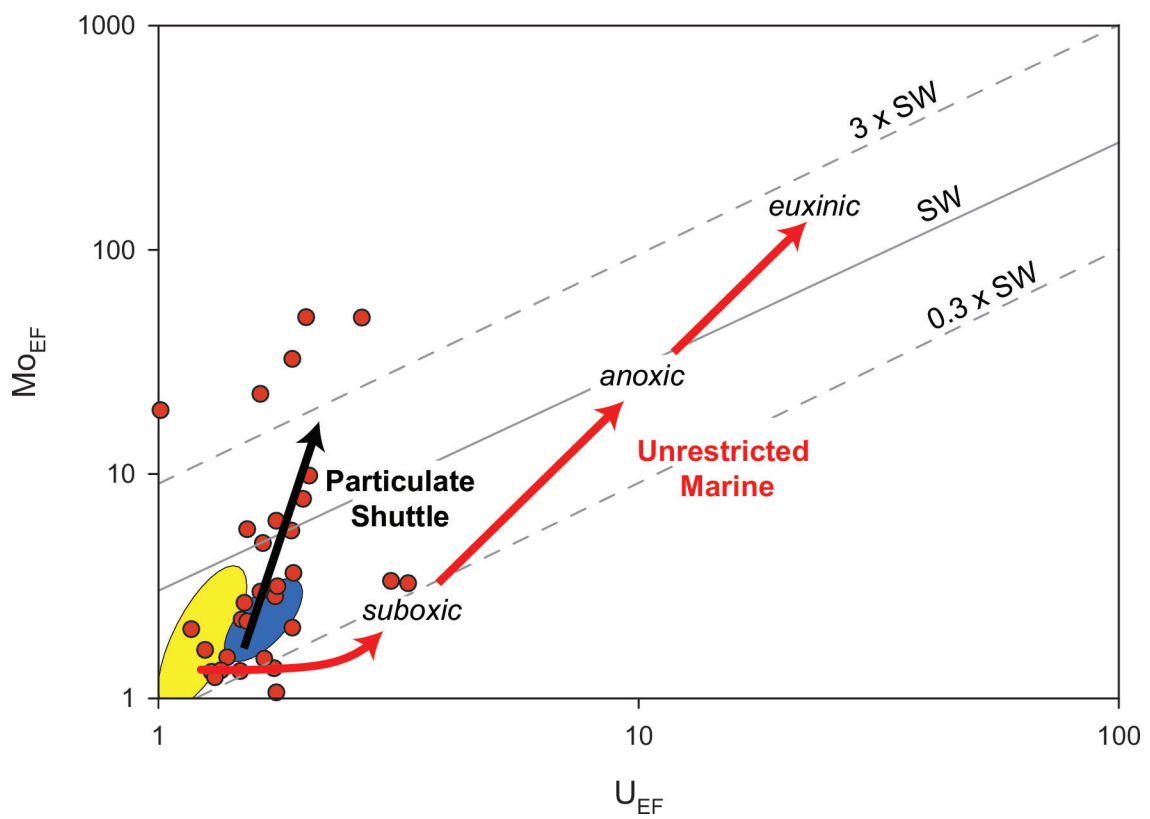
2019gl083316-f01-z-.eps



2019gl083316-f02-z-eps



2019gl083316-f03-z-eps



2019gl083316-f04-z-eps